



OPEN ACCESS

EDITED BY

Etel Rocha-Vieira,
Universidade Federal dos Vales do
Jequitinhonha e Mucuri, Brazil

REVIEWED BY

Yadira Palacios,
Metropolitan Autonomous University, Mexico
Christopher Urbschat,
University Medical Center Hamburg-
Eppendorf, Germany

*CORRESPONDENCE

Lucile E. Wrenshall
✉ lucile.wrenshall@wright.edu

†PRESENT ADDRESS

Kristie N. Dinh,
Fertility Wellness Institute of Ohio West
Chester Township, Dayton, OH, United States

RECEIVED 13 January 2024

ACCEPTED 17 April 2024

PUBLISHED 15 May 2024

CITATION

Wong VA, Dinh KN, Chen G and Wrenshall LE
(2024) IL-2R α KO mice exhibit maternal
microchimerism and reveal nuclear
localization of IL-2R α in lymphoid
and non-lymphoid cells.
Front. Immunol. 15:1369818.
doi: 10.3389/fimmu.2024.1369818

COPYRIGHT

© 2024 Wong, Dinh, Chen and Wrenshall. This
is an open-access article distributed under the
terms of the [Creative Commons Attribution
License \(CC BY\)](#). The use, distribution or
reproduction in other forums is permitted,
provided the original author(s) and the
copyright owner(s) are credited and that the
original publication in this journal is cited, in
accordance with accepted academic
practice. No use, distribution or reproduction
is permitted which does not comply with
these terms.

IL-2R α KO mice exhibit maternal microchimerism and reveal nuclear localization of IL-2R α in lymphoid and non-lymphoid cells

Victoria A. Wong¹, Kristie N. Dinh^{2†}, Guangchun Chen³
and Lucile E. Wrenshall^{1,4*}

¹Department of Neuroscience, Cell Biology, and Physiology, Boonshoft School of Medicine, Wright State University, Dayton, OH, United States, ²Fertility Wellness Institute of Ohio West Chester Township, OH, United States, ³Genomics and Microarray Core Facility, University of Texas Southwestern Medical Center Dallas, TX, United States, ⁴Department of Medical Education, Boonshoft School of Medicine, Wright State University, Dayton, OH, United States

Introduction: IL-2R α knock out (KO) mice have been instrumental to discovering the immunoregulatory properties of IL-2R α . While initially thought of only as a stimulatory cytokine, IL-2 and IL-2R α KO mice revealed that this cytokine-receptor system controls immune responses through restimulation-induced cell death and by promoting the survival of T regulatory cells. Although described mostly in the context of lymphocytes, recent studies by our laboratory showed that IL-2R is expressed in smooth muscle cells. Given this finding, we sought to use IL-2R α KO to determine the function of this receptor in vascular smooth muscle cells. Surprisingly, we found that IL-2R α KO vascular smooth muscle cells had detectable IL-2R α .

Methods: We used multiple gene and protein-based methods to determine why IL-2R α KO vascular smooth muscle cells exhibited IL-2R α protein. These methods included: genomic sequencing, assessing cells and tissues for evidence of maternal microchimerism, and determining the half-life of IL-2R α protein.

Results: Our studies demonstrated the following: (1) in addition to the cell surface, IL-2R α is localized to the nucleus; (2) the genetic deletion of IL-2R α is intact in IL-2R α KO mice; (3) both IL-2R α KO and WT tissues show evidence of maternal microchimerism, the likely source of IL-2R α (4) IL-2R α is transmitted between cells; (5) IL-2R α has a long half-life; and (6) nuclear IL-2R α contributes to the regulation of cell proliferation and size.

Conclusion: Our findings suggest that the phenotype of complete IL-2R α loss is more severe than demonstrated by IL-2R α KO mice, and that IL-2R α plays a heretofore unrecognized role in regulating cell proliferation in non-lymphoid cells.

KEYWORDS

IL-2R α , maternal microchimerism, knock out, nucleus, cell proliferation, cell size, vascular smooth muscle cells

Introduction

IL-2R α , or CD25, is a key subunit of the tripartite IL-2 receptor. Expression of IL-2R α distinguishes activated from naïve T cells, and high expression serves as a marker for T regulatory cells. The contribution of IL-2R α to T regulatory cell survival and prevention of autoimmunity has been demonstrated through IL-2R α knock out (KO) mice, which develop splenomegaly, lymphadenopathy, anemia, and inflammatory bowel disease (1, 2). IL-2R α KO mice have been instrumental in determining the impact of IL-2R α on the immune system (1, 3–5).

Although the IL-2R is best known for its expression on lymphocytes, there are limited reports demonstrating the expression of IL-2R on other cell types, particularly dendritic cells (6–8). Our laboratory recently reported that vascular smooth muscle cells (VSMC) express all 3 subunits of the IL-2R (9). We found that expression of the IL-2R α differed with VSMC phenotype, with proliferating VSMC expressing lower levels of IL-2R α than differentiated VSMC.

To help define the function of IL-2R α in VSMC, we sought to study cell properties in the absence of IL-2R α . To this end, we isolated VSMC from IL-2R α wildtype (WT) and KO mice. Surprisingly, we found that IL-2R α protein was present, mainly in the nucleus, of both WT and KO VSMC. IL-2R α was detected in IL-2R α KO VSMC and splenocytes by immunofluorescence, flow cytometry, and Western blot analysis. Low levels of WT *IL2RA* were detected in genomic DNA extracted from multiple IL-2R α KO tissues. Our studies suggest that the source of *IL2RA* DNA, and in turn IL-2R α protein, is maternal microchimerism. The magnitude and pervasive nature of the IL-2R α protein in KO mice is likely due to our finding that IL-2R α protein has a surprisingly long half-life, and that IL-2R α protein can be transferred between cells.

Materials and methods

Materials and animals

Animal studies were approved by the Institutional Animal Care and Use Committee at Wright State University and conformed to the Guide for the Care and Use of Laboratory Animals (NIH Publication, 8th edition). Heterozygous breeding pairs of IL-2R α null (B6;129S4-*IL-2ra*^{tm1Dw}/J) mice were purchased from The Jackson Laboratory (Bar Harbor, ME, USA) for the establishment of breeding colonies (1).

Antibodies recognizing IL-2R α were from the following sources: rabbit anti-human polyclonal anti-IL-2R α antibodies were from Bioss Antibodies, Inc. (Woburn, MA), BosterBio (Pleasanton, CA), and LSBio (Seattle, WA). Mouse anti-human and anti-mouse IL-2R α , clone 1B5D12, was from Genetex (Irvine, CA). Epitopes for these antibodies are as follows: Bioss aa 258–268; BosterBio aa 39–57; LSBio aa 223–272; Genetex aa 34–139. Rabbit anti-phospho-CD25 (ser268) was from Sigma (St. Louis, MO). Rat anti-mouse CD16/32, rat anti-mouse CD4, and rat anti-mouse IL-2R α (clone PC61) were from Biolegend (San Diego, CA). Purified mouse IL-2R α was from SinoBiological (Wayne, PA). Antibodies

used for SMC identification were as follows: rabbit anti-human smooth muscle cell alpha actin was from Novus (Littleton, CO). Sheep anti-transgelin (multiple species) was from R&D Systems (Minneapolis, MN). Rabbit anti-human h-caldesmon was from Proteintech (Rosemont, IL). Benzonase[®] was from Minnebio (St. Paul, MN). DMEM was from ThermoFisher (Waltham, MA).

VSMC culture

Murine VSMC were isolated from thoraco-abdominal aortas by enzymatic digestion based on a protocol from Kwartler, et al. (10). Aortas were dissected free of adipose tissue *in situ*, removed and rinsed three times in sterile Hanks' balanced salt solution, then digested at 37°C for 16–18h with a mixture of 0.1 mg/ml collagenase (Sigma), 25 μ g/ml trypsin inhibitor (Sigma) and 18 μ g/ml elastase (Worthington Biochemical Corp., Lakewood, NJ). Isolated smooth muscle cells and any remaining tissues were then washed and cultured in DMEM with 10% FBS at 37°C and 5% CO₂. Tissue debris was removed the following day.

For serum free conditions, VSMC were cultured in DMEM supplemented with insulin, transferrin, and selenium (ITS; Sigma) (11). Identification of cells as VSMC was confirmed through expression of smoothelin (passage 1–2 only), smooth muscle cell α -actin, transgelin, and h-caldesmon.

Human VSMC were isolated from pieces of aorta using the explant technique (9). Tissues were washed with PBS and all adipose was removed. The artery was then cut into small (approximately 5 mm x 5 mm) pieces and 2–3 pieces per well were placed lumen side down into 6 well tissue culture plates. Pieces were allowed to adhere briefly, then smooth muscle cell media (ScienCell, Carlsbad, CA) supplemented with 10% FBS was carefully added to the wells so as not to dislodge the pieces of aorta. The tissue was maintained at 37°C and SMCs were harvested in 3–4 weeks. VSMC were then passaged every 7–8 days and used after 1–2 passages.

PCR and qPCR

Offspring of heterozygous breeding pairs of IL-2R α null (B6;129S4-*IL-2ra*^{tm1Dw}/J) mice were genotyped per Jax mice touchdown protocol (12). Briefly, DNA was extracted from tail clippings and amplified using the recommended primers and touchdown protocol. Primers were as follows: (WT forward CTGTGTCTGTATGACCCACC, WT reverse CAGGAGTTTCCTAAGCAACG; mutant forward CTTGGTGAGAGGCTATTC, mutant reverse AGGTGAGATGACAGGAGATC). The WT primer sequences are contained within exon 2.

Quantitative real time PCR was performed, using the above primers, with 15 ng genomic DNA input in triplicate on a 7500 fast real-time PCR system (Applied Biosystems, ThermoFisher Scientific) using PowerUp[™] SYBR[™] Green Master Mix kit (Applied Biosystems) according to the manufacturer's instructions. The cycle profile was 2 minutes at 50°C, 2 minutes at 95°C, 40 cycles of 3 seconds at 95°C and 30 seconds at 60°C. GAPDH was used as an endogenous control. RT-minus and no

template controls (NTC) were included for negative control. Data were analyzed using 7500 software v2.3 (Applied Biosystems).

Flow cytometry

Splenocyte cell suspensions were prepared by mechanical disruption of the spleen followed by filtration to remove large pieces of noncellular debris. The following incubations were all performed on ice. Splenocytes were first incubated with anti-CD16 (TruStain, FcX) for 15 min, then washed and stained with the indicated anti-IL-2R α antibodies for 30 minutes. Following fixation in 2% paraformaldehyde, intracellular staining was performed by first permeabilizing cells via suspension in ice cold methanol for 30 minutes. Cells were then washed twice in PBS with 2% BSA and stained with anti-IL-2R α antibodies for 30 minutes. Clone PC 61.5 and anti-IL-2R α from Genetex were directly conjugated to Cy-5 fluorochromes and anti-IL-2R α from Boster was used with a Cy5 labeled secondary antibody. A subset of cells was treated with Benzonase[®] 250U/10⁶ cells for 50 minutes at 37°C prior to staining. Data were acquired on a Accuri C6 flow cytometer (Bectin Dickinson, Franklin Lakes, NJ) and analyzed using FCS Express 7 (Pasadena, CA).

Microscopy

VSMC were cultured in chamber slides and fixed in ice cold methanol with 2% acetic acid. Fixed VSMC were then washed with PBS and blocked for 1h using Odyssey blocking solution (LI-COR, Lincoln, NE). Blocking solution was removed by washing, and primary antibodies were diluted in TBST (10 mM Tris, pH 8.0, 150 mM NaCl, 0.5% Tween 20) and applied to cells overnight at 4°C. The primary antibody was removed by washing, and the appropriate fluor-conjugated secondary was applied for 1h. Cells were imaged on an EVOS epifluorescent microscope (ThermoFisher) or on a Cytation imaging plate reader (Biotek, Winooski, VT). Images from the Cytation were processed using the flow cytometry software FCS Express 7.

Western blot analysis

Whole cell lysates from primary VSMCs and Jurkat T cells (ATCC, Manassas, VA) were prepared by lysing and sonicating pelleted cells in radio immuno-precipitation (RIPA) buffer (150 mM NaCl, 25 mM Tris-HCl pH 7.6, 1% Nonidet P40, 1.0% sodium deoxycholate, 0.1% SDS). Splenocytes were separated into membrane, cytoplasmic, and nuclear fractions per manufacturer's instructions (Cell Fractionation Kit, Cell Signaling Technology, Danvers, MA). Extracts were then separated by SDS-PAGE, using 30 μ g protein measured by bicinchoninic acid assay (Pierce, Thermo-Fisher), and transferred to a polyvinylidene difluoride membrane. Some blots, as indicated in figure legends, were assessed for total protein using either stain-free gels (Bio-Rad, Hercules, CA) or the Revert[™] 700 Total Protein Stain (LI-COR) prior to blocking. After incubation with 5% nonfat milk in TBST for

60 min, the membrane was incubated with antibodies against IL-2R α at 4°C for 18 h. Membranes were washed three times for 10 min and incubated with a 1:10,000 dilution of horseradish peroxidase-conjugated anti-rabbit antibodies (Jackson ImmunoResearch, West Grove, PA) at room temperature for 2 hrs. Blots were washed with TBST three times and developed with the ECL system (Luminata Crescendo, Millipore Sigma) according to the manufacturer's instructions.

Protein half-life

The half-life of IL-2R α was measured using a protocol designed by Morey, et al. (13) in which a traditional pulse-chase experiment was performed using L-azidohomoalanine (AHA), a methionine analog, as the pulsed label. Incorporation of AHA into nascent proteins was detected by a click chemistry based, copper-free strain-promoted alkyne-azide cycloaddition reaction in which a fluorescent cyclooctyne probe (dibenzocyclooctyne-488) bound to incorporated AHA (14, 15).

Specifically, VSMC were washed then cultured in methionine free DMEM with 5% dialyzed FBS containing 50 μ M L-azidohomoalanine (AHA) for 48 hours (duration determined by pilot experiments) then cells were returned to DMEM with 10% FBS. VSMC were pelleted at indicated time intervals following this initial pulse and then processed together. Because IL-2R α is primarily localized to the nucleus in VSMC, we focused on extracting nuclear proteins. Nuclear fractions were isolated following the protocol outlined by Senichkin, et al. (16). Briefly, pelleted cells were incubated in a hypotonic buffer (20 mM Tris-HCl (pH 7.4), 10 mM KCl, 2 mM MgCl₂, 1 mM EGTA, 0.5 mM DTT, 0.5 mM PMSF) for 3 minutes, followed by addition of 0.1% NP-40 (final concentration) for an additional 3 minutes. Following centrifugation, the pellet was incubated in isotonic buffer (20 mM Tris-HCl (pH 7.4), 150 mM KCl, 2 mM MgCl₂, 1 mM EGTA, 0.5 mM DTT, 0.5 mM PMSF) plus 0.1% NP-40 for another 3 minutes, then centrifuged. The resulting nuclear pellet was resuspended in 100 μ l Benzonase[®], 100U for 10 minutes at 37°C. RIPA buffer, 400 μ l, was then added for 20 minutes at room temperature (RT). Following centrifugation, the supernatant (nuclear soluble fraction) was saved and the insoluble pellet, if present, was washed and resuspended in 100 μ l Benzonase[®] 100 U. Following a 10-minute digestion at 37°C, the digested lysate was combined with the nuclear soluble fraction for immunoprecipitation, labeling with dibenzocyclooctyne (DBCO)-488, and Western blot analysis.

DBCO labeling and immunoprecipitation were performed as follows. Prepared lysates were heated at 95°C for 10 minutes to denature proteins and increase access to internal AHA-bearing sequences. Iodoacetamide 10 mM, which decreases azide-independent labeling, was added to cooled lysates for 30 minutes at RT (17). Lysates were then immunoprecipitated using anti-IL-2R α antibody directly conjugated to magnetic beads. Conjugation was performed per manufacturer's instructions (Click-&-Go, Click Chemistry Tools, Scottsdale, AZ). Following a 1h incubation at RT, beads (now containing bound protein) were washed and incubated with 5 μ M DBCO-488 (Click Chemistry Tools) for 30 min at RT or

overnight at 4°C. Beads were washed again and labeled protein was eluted with lithium dodecyl sulfate (LDS) containing sample buffer in preparation for SDS-PAGE.

Levels of DBCO-labeled IL-2R α were normalized using either total protein (Revert™ 700 Total Protein Stain) or total IL-2R α detected by either the anti-IL-2R α antibody from BosterBio or anti-phospho-CD25 (ser268). The latter antibody was chosen for its strong signal and suggests that IL-2R α is active. A linear regression analysis was then performed on normalized levels of labeled IL-2R α and half-life was calculated via the following equation: $t_{1/2} = \ln(2)/\text{slope of decay}$ (13).

Statistics

Groups were compared using an unpaired, two-tailed t test with Welch's correction. P values in figures are defined as follows: ns P > 0.05; * P ≤ 0.05; ** P ≤ 0.01; *** P ≤ 0.001; **** P ≤ 0.0001.

Results

IL-2R α KO VSMC express IL-2R α protein

To determine how IL-2R α affects the function of VSMC, we isolated VSMC from IL-2R α KO and WT mice. WT and KO mice were genotyped using the protocol provided by JAX® (18). As a first step following isolation and culture, we examined expression of IL-2R α protein in WT and KO VSMC by indirect immunofluorescence. VSMC isolated from WT mice expressed IL-2R α primarily in the nucleus, consistent with our recent observations in human VSMC (Figures 1A, B). However, IL-2R α was also detected in the nucleus of VSMC isolated from IL-2R α KO mice. Similar results were obtained with antibodies from multiple sources. Although most antibodies detected IL-2R α in the nucleus, two antibodies showed partial (Bioss) or predominantly (Genetex) membrane or cytoplasmic localization (Figure 1A, Supplementary Figure 1). Although we have not established the reason behind this differential detection, it likely relates to the fact that IL-2R α is heavily glycosylated which may obscure some epitopes. Pre-adsorption with a known peptide epitope, available for the antibody obtained through BosterBio, abrogated staining (Figure 1C).

Membrane IL-2R α is known to be cleaved by different proteases, at approximately amino acid 192, into a soluble form (19, 20). Because antibodies from LSBio and Bioss recognize epitopes within the C terminus (see Methods for epitopes), and because IL-2R α from distinct cell fractions are equal in size (Figure 2C) this demonstrates that the nuclear form of IL-2R α is full length and not present through uptake of the soluble form.

IL-2R α KO mice were generated by replacing exons 2 and 3 of IL-2R α with a neomycin resistance gene (1). IL-2R α is known to have multiple splice variants – three have been identified in mouse IL-2R α and nine in human IL-2R α (21). To ensure that the IL-2R α

protein detected was not produced by a splice variant, potentially excluding the neomycin resistance insert, we assessed the size of IL-2R α protein produced by WT and KO VSMC using Western blot analysis. As seen in Figure 1D, WT and IL-2R α KO VSMC expressed IL-2R α of the same size, identical to that of human VSMC and Jurkat T cells (9). These results suggest that IL-2R α KO VSMC express full-length IL-2R α .

IL-2R α KO splenocytes express IL-2R α protein

Because IL-2R α expression and function are mainly studied in T cells, we asked whether lymphocytes from IL-2R α KO mice express IL-2R α protein. To this end, we isolated splenocytes from WT and IL-2R α KO mice and examined IL-2R α expression by flow cytometry in the presence or absence of stimulation with phytohemagglutinin (PHA) to upregulate membrane IL-2R α . Since IL-2R α appears mainly localized to the nucleus in VSMC, we also permeabilized cells to look for nuclear expression. To assess IL-2R α expression, we used two of the same antibodies used in VSMC, sourced from Genetex and BosterBio (see Figure 1).

In non-permeabilized cells, a subset of WT splenocytes expressed IL-2R α on their cell surface when stimulated with PHA (Figure 2A). A small subset of KO cells also expressed IL-2R α . Upon permeabilization, however, IL-2R α was detected by in the majority of WT splenocytes (70-80%). IL-2R α was also detected in permeabilized KO splenocytes, however the frequency was lower than in WT cells, particularly those stained with the anti-IL-2R α from Genetex. The intensity of staining was also decreased in permeabilized KO vs WT splenocytes (Figure 2B).

These results suggested that IL-2R α could be localized to the nucleus in lymphocytes. To address this question, we separated splenocyte lysates into membrane, cytoplasm, and nuclear fractions. Consistent with our findings in VSMC, IL-2R α was present in the nucleus (Figure 2C).

We then asked whether a commonly used anti-IL-2R α antibody, rat anti-mouse IL-2R α clone PC61.5, yielded similar results (22–25). Non-permeabilized WT splenocytes stimulated with PHA yielded strong expression, as expected, and similarly treated KO cells were negative (Figure 3A). However, permeabilization yielded only low levels of IL-2R α in WT cells and KO cells were negative. Given the nuclear localization of IL-2R α (Figures 1, 2), we reasoned that a potential association with DNA might be blocking some epitopes. To test this question, we digested permeabilized cells with Benzonase®, a genetically engineered endonuclease that degrades all forms of DNA and RNA. IL-2R α was strongly detected in permeabilized WT and KO splenocytes following Benzonase® digestion, although the level of expression per cell (mean channel fluorescence) was much higher in WT cells (Figure 3B). Pre-adsorption of PC61.5 with purified mouse IL-2R α protein abrogated this staining (Figure 3A).

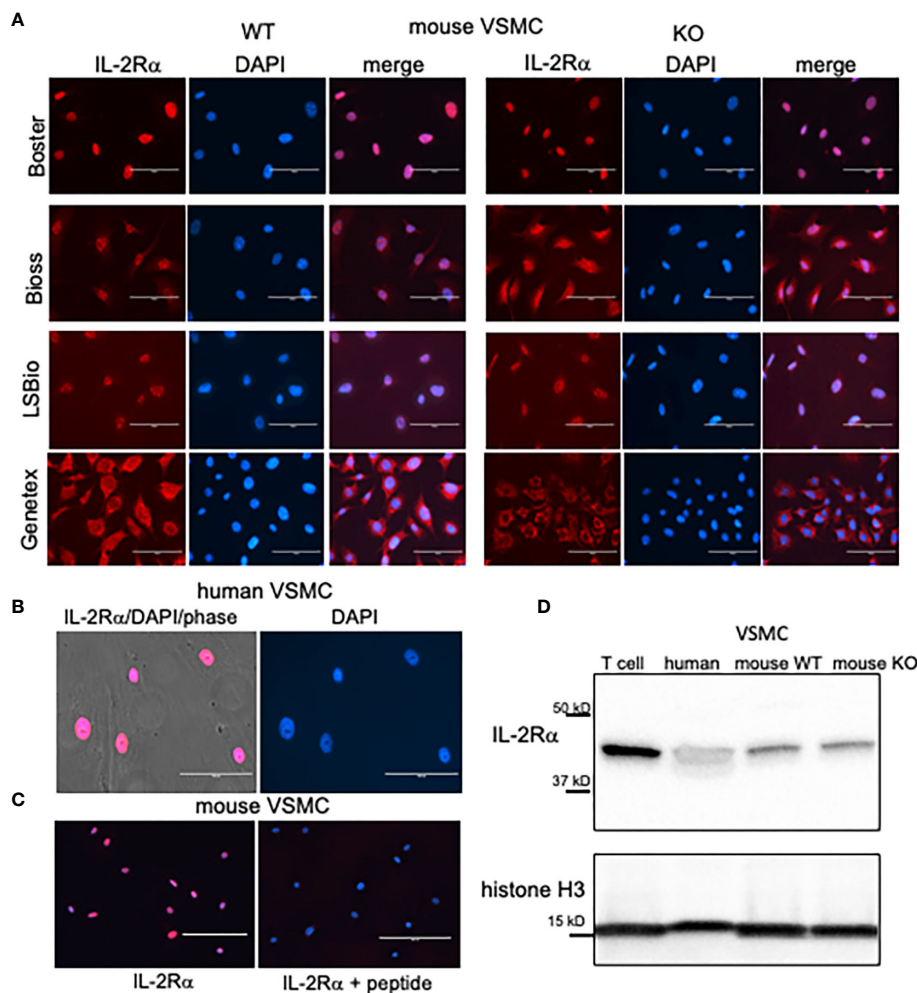


FIGURE 1

VSMC isolated from IL-2R α KO mice express IL-2R α protein. (A) VSMC, isolated from IL-2R α WT and KO mice, were cultured to 60–70% confluency. After fixation and blocking, primary antibodies recognizing IL-2R α , purchased from various sources as indicated, were applied to VSMC followed by the appropriate Cy5 conjugated secondary. Cells were imaged using an EVOS FL epifluorescence microscope (ThermoFisher Scientific). Scale bar = 100 μ . (B) Human VSMC were stained with the anti-IL-2R α from BosterBio. Scale bar = 100 μ . (C) Murine VSMC were stained as in (A) using anti-IL-2R α from Boster with/without pre-adsorption with immunizing peptide. Scale bar = 200 μ . (D) Lysates of VSMC or Jurkat T cells were separated by SDS-PAGE and analyzed for expression of IL-2R α , using anti-IL-2R α from Boster. Histone H3 was used as a loading control. Results shown are representative of >5 (A, B), 3 (C), and >5 (D) separate experiments.

Although prior attempts at using clone PC61.5 to detect IL-2R α in VSMC yielded poor results, based on the above findings we digested methanol-fixed VSMC with Benzonase[®]. Digestion of mouse VSMC with Benzonase[®] allowed for the detection of IL-2R α in the nucleus, consistent with our findings in T cells (Figure 3C). In addition, these results suggest that at least a portion of nuclear IL-2R α binds DNA.

Genomic sequencing demonstrates *IL2RA* deletion

In light of our results demonstrating that both IL-2R α KO splenocytes and VSMC produce IL-2R α , we sought to establish its source. As a first step, we asked if the deletion in the *IL2RA* gene was intact. To this end, we sequenced genomic DNA isolated from WT

and KO VSMC. Targeted genome sequencing of the *IL2RA* gene from KO cells revealed correct deletion of exons 2 and 3 as initially reported by Willerford, et al. (1) (Figure 4).

Multiple tissues in IL-2R α KO mice have low levels of the *IL2RA* gene

Given that *IL2RA* was correctly deleted, we considered other sources of the WT gene. One potential source of the WT *IL2RA* gene is maternal transfer. Maternal microchimerism, the transfer of cells from mother to fetus, is well established in humans and mice wherein maternal DNA/cells can persist for decades in offspring (26–30). Because IL-2R α KO mice are infertile, they are generated by mating IL-2R α heterozygotes; consequently, heterozygous maternal cells are likely present in IL-2R α KO mice. Maternal

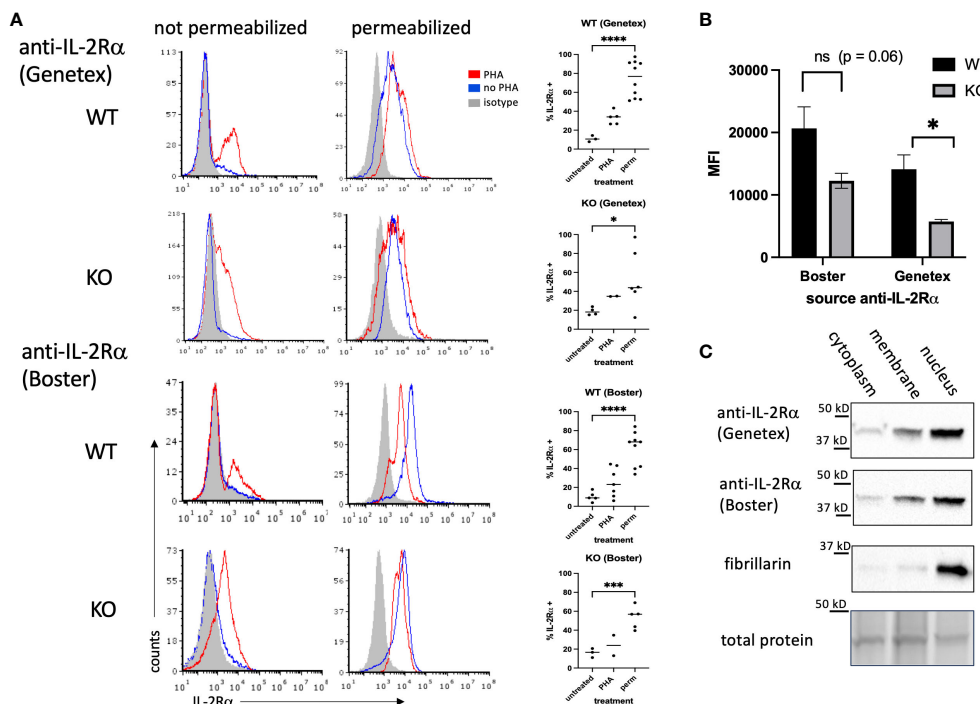


FIGURE 2

IL-2R α is detectable in the nucleus of IL-2R α WT and KO splenocytes. (A) Splenocytes, prepared fresh (untreated/no PHA) or following 48h of stimulation with PHA 10 μ g/ml, were stained with anti-IL-2R α antibodies or isotype controls as indicated with/without first permeabilizing via methanol. Graphs to the right of histograms represent a summary of individual values from multiple experiments. Permeabilized (perm) groups with/without PHA were combined. (B) represents the average MFIs \pm SEM, derived from (A), of permeabilized splenocytes stained with anti-IL-2R α antibodies as indicated. (C) Splenocytes were stimulated with PHA for 48h, pelleted and fractionated into membrane, cytoplasm, and nuclear fractions, then analyzed by Western blot probing with antibodies as indicated. Blots represent lysates processed in parallel. Total protein, obtained from stain-free gels (Bio-Rad), shows the single most prominent band present across all samples. Results shown are representative of ≥ 3 experiments. * $P \leq 0.05$; *** $P \leq 0.001$; **** $P \leq 0.0001$.

microchimerism may therefore represent result a potential source of IL-2R α in KO offspring of heterozygous females. Our laboratory previously demonstrated that maternal microchimerism was responsible for the presence of IL-2 in IL-2 KO mice, which obscured severe defects in thymic development (29).

Using the *IL2RA* gene as an indicator of maternal microchimerism, we extracted genomic DNA from IL-2R α KO tissues and looked for evidence of *IL2RA*, using primers that amplify a segment within exon 2 that should be absent in KO mice (1). Relative levels of *IL2RA* were assessed by qPCR of genomic DNA. QPCR of maternal markers in genomic DNA of offspring has been used by other investigators to detect maternal microchimerism (26). As seen in Figure 5A, 6/6 spleens, 6/6 kidneys, and 3/3 hearts from adult KO mice had detectable (RQ > 0 with one of the KO spleens as reference) levels of *IL2RA*. As further evidence for the presence of maternal cells in offspring of IL-2R α het breeders, we assessed spleens from IL-2R α WT offspring of heterozygous parents for the neomycin resistance gene used in the generation of IL-2R α KO mice. Five of five spleens tested had detectable levels of the *NeoR* gene (Figure 5B). As expected, control spleens from unrelated mice that were not offspring of IL-2R α het mice had no detectable *NeoR* gene.

G418 decreases IL-2R α protein detected in IL-2R α KO VSMC

As previously mentioned, IL-2R α KO mice were generated by replacing exons 2 and 3 of IL-2R α with a neomycin resistance gene insert as a selectable marker (1). If IL-2R α KO VSMC contained low numbers of IL-2R α heterozygous cells, as our results suggest, then treatment with neomycin might eliminate these cells if they are less resistant to neomycin than KO cells. In turn, IL-2R α protein expression should decrease. To test this hypothesis, we cultured WT and KO VSMC with increasing concentrations of G418 (a neomycin analog). G418 nearly eliminated WT cells at a concentration of 2 mg/ml (Figure 6A). However, many VSMC isolated from KO mice survived this treatment. IL-2R α production by these cells following treatment with G418 was significantly diminished compared to untreated VSMC isolated from IL-2R α KO mice as shown by both immunofluorescence and Western blot analysis (Figures 6A-C). These data suggest that the neomycin resistance protein is expressed and functional in IL-2R α KO VSMC, and that treatment of KO VSMC with G418 decreased IL-2R α protein originating from heterozygous cells.

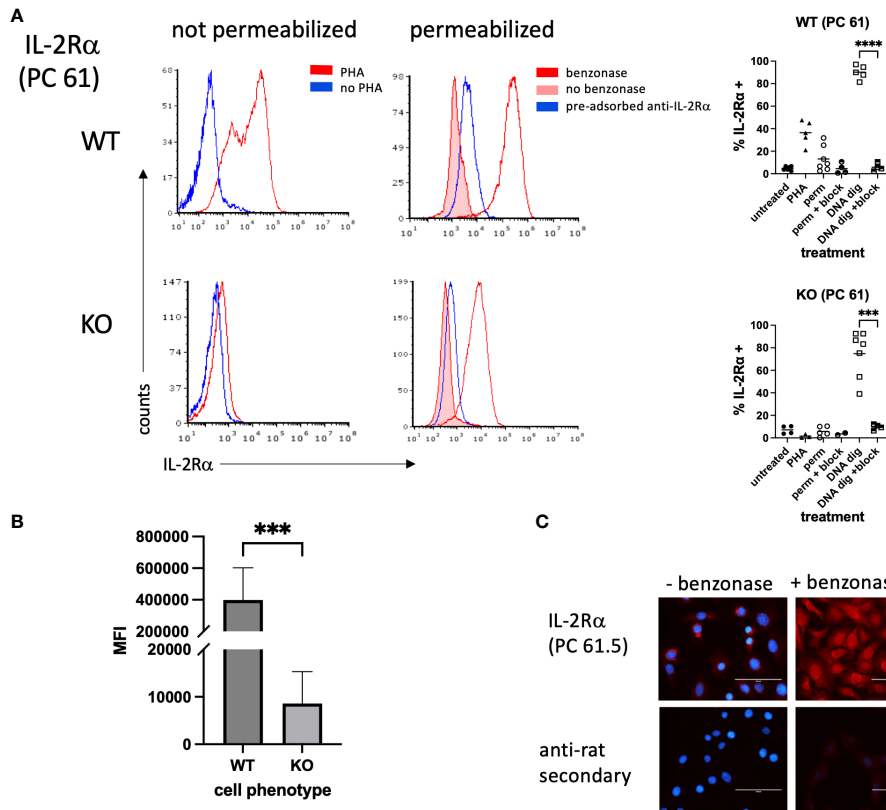


FIGURE 3
 IL-2R α is detected in permeabilized splenocytes by rat anti-mouse IL-2R α (clone PC 61) following DNA digestion. **(A)** Splenocytes were prepared as described in **Figure 2**. A subset of methanol permeabilized cells were treated with Benzonase[®] 250U/10⁶ cells or enzyme buffer for 50 minutes at 37°C prior to staining. In a subset of samples, anti-IL-2R α /clone PC 61 was pre-adsorbed with an excess of purified mouse IL-2R α . Graphs to the right of histograms represent a summary of individual values from multiple experiments. "Block" indicates use of pre-adsorbed anti-IL-2R α . **(B)** represents the average MFIs \pm SEM, derived from **(A)**, of permeabilized splenocytes treated with Benzonase[®]. **(C)** VSMC were permeabilized with methanol and treated with Benzonase[®] or buffer, as indicated above, then stained with anti-IL-2R α /clone PC 61. Note that digestion with Benzonase[®] eliminates DAPI staining as expected. Scale bar = 100 μ . *** P \leq 0.001; **** P \leq 0.0001.

IL-2R α protein is transferred between cells

Although our first attempt at clearance of IL-2R α protein by treatment with G418 significantly decreased IL-2R α protein expression, we were unable to eliminate IL-2R α despite ongoing treatment with G418 and/or increased dosage (**Figure 7**). Upon

performing formal kill curves with G418, we observed that the difference in resistance between heterozygous and homozygous cells is probably not large enough to differentially eliminate all heterozygous cells (**Supplementary Figure 2**).

As part of efforts to identify the source of ongoing IL-2R α production, we noted that VSMC were heterogeneous in size, and

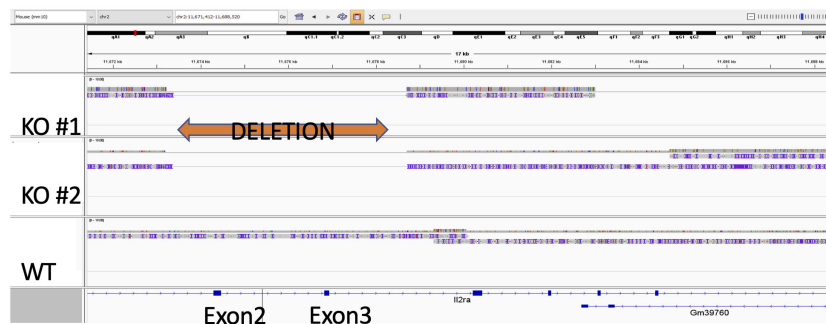


FIGURE 4
 Exons 2 and 3 of IL-2R α gene are deleted in IL-2R α KO mice. Genomic DNA isolated from WT and KO VSMC underwent targeted sequencing, with a focus on the IL-2R α locus. Exons 2 and 3 of IL-2R α are deleted as reported by Willerford, et al. (1).

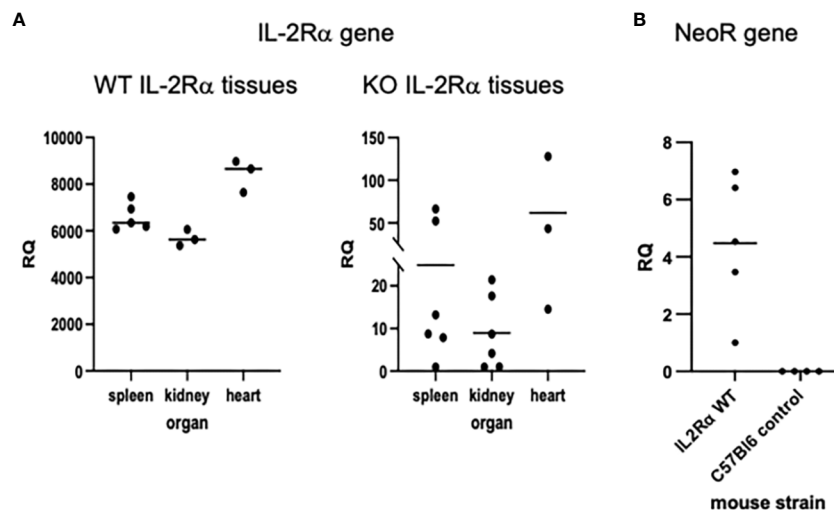


FIGURE 5

IL-2R α gene is present in IL-2R α KO tissues. Genomic DNA was isolated from various organs as indicated. Levels of *IL2RA* (A) or *Neo* resistance (B) DNA were measured in each tissue by qPCR. The relative quantity (RQ) of *IL2RA* or *Neo* DNA was measured relative to a single KO spleen (A) or a WT spleen (B).

that large cells appeared to express high levels of IL-2R α protein (Figure 7A). Using filters (Pluriselect, Leipzig, Germany), we separated cells into those that passed through a 1 micron filter from the remainder that did or did not pass through a 30 micron filter. We then compared levels of *IL2RA* DNA amongst these cells and with those that had not received G418. As seen in Figure 7B, larger cells contained relatively more *IL2RA* DNA than smaller

cells, and those without G418 treatment contained the most *IL2RA* DNA, consistent with our observations of IL-2R α protein expression (Figures 6, 7).

Given the above findings, combined with our observation that most VSMC isolated from IL-2R α KO mice expressed at least low levels of IL-2R α protein, we asked whether IL-2R α could be transferred between cells. To this end, we co-cultured IL-2R α KO

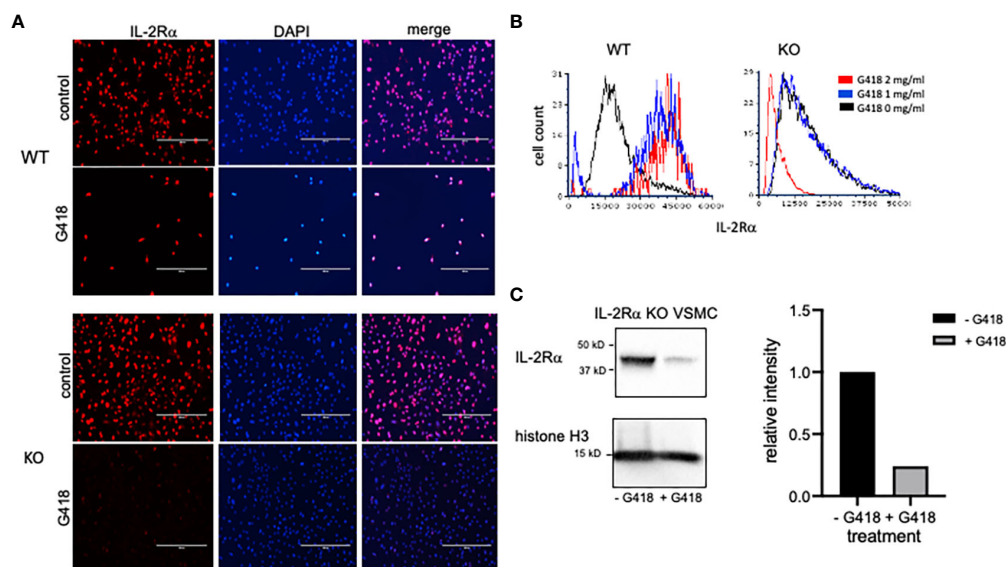


FIGURE 6

G418 decreases IL-2R α protein detected in VSMC isolated from IL-2R α KO mice. (A) VSMC, isolated from IL-2R α WT and KO mice, were cultured in the presence/absence of G418 at 2 mg/ml. Cells were probed for IL-2R α expression using the anti-IL-2R α from Boster as described in Figure 1. Scale bar = 400 μ . (B) The intensity of IL-2R α staining in all cells from (A) was measured in an image cytometer and converted to a histogram using flow cytometry software. To highlight differences in fluorescence intensity, histograms were normalized to peak values of WT or KO cells at 0 mg/ml G418. Cell numbers analyzed, in order from 0 – 2 mg/ml G418, were as follows: WT 7425, 911, 218; KO 7621, 9941, 7656. (C) KO VSMC, cultured as described in (A), were lysed. Extracted proteins were separated by SDS-PAGE and analyzed by Western blot for expression of IL-2R α using the anti-IL-2R α antibody from Boster. Intensity of the IL-2R α band from each treatment was expressed as a ratio of IL-2R α /histone H3. Densitometry was performed using Image Lab software from Bio-Rad Laboratories. Results shown for (A, C) are representative of >3,2 separate experiments respectively.

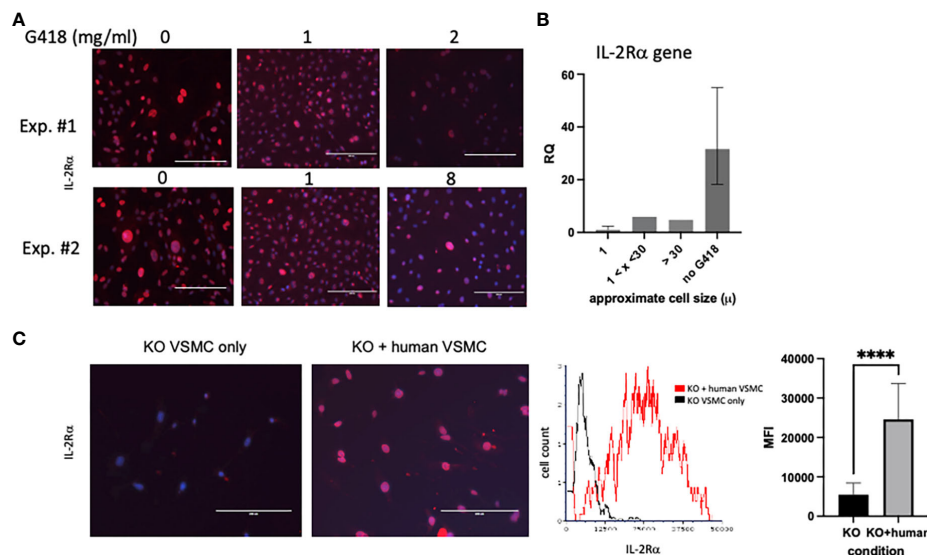


FIGURE 7

IL-2R α is transferred between cells. (A) VSMC were cultured for 96h with increasing concentrations of G418 as indicated. IL-2R α protein expression was detected using the anti-IL-2R α antibody from BosterBio. (B) VSMC, cultured in G418, were separated by size using 1 and 30 micron filters as indicated. Genomic DNA was isolated from cell pellets and levels of *IL2RA* DNA were quantified relative to the 1 micron cells. (C) Human VSMC were placed in transwell inserts and co-cultured with murine VSMC for 96h and compared to murine VSMC without co-culture. IL-2R α protein expression was detected using the anti-IL-2R α antibody from BosterBio. Intensity of IL-2R α staining in all cells was measured in an image cytometer (Cytation) then converted to a histogram or bar graph using flow cytometry or data analysis software. Scale bar = 200 μ . **** $P \leq 0.0001$.

VSMC with human VSMC using a transwell insert, in which human VSMC were suspended over KO VSMC and separated by a filter. We chose human VSMC for their robust IL-2R α protein expression (Figure 1). IL-2R α was easily detectable in IL-2R α KO VSMC that had been co-cultured with human VSMC, compared to those that were not (Figure 7C). These results suggest that IL-2R α protein is transferred between cells by a means not requiring cell contact, likely through extracellular vesicles such as exosomes or apoptotic bodies (31, 32).

Half-life of IL-2R α

While the previous results suggest that IL-2R α protein present in KO mice originated from maternal microchimerism, the low levels of *IL2RA* DNA detected did not seem consistent with the comparatively high levels of protein. One way in which protein levels may be regulated is through their half-life. In a recent report by Chen, et al, a systematic study of half-lives of proteins in human HepG2 cells showed that most proteins had half-lives ranging from 4-14 hours (33).

Given the easily detectable IL-2R α protein evident in KO mice, we hypothesized that the half-life of IL-2R α is long, likely days versus hours. To measure the half-life of IL-2R α , we performed a pulse chase experiment, in which we labeled newly synthesized proteins with a methionine analog, AHA, then assessed their degradation over time through loss of labeled proteins. Incorporated AHA was detected by fluorescently labeled DBCO, which binds the azido group in AHA through strain promoted alkyne-azide cycloaddition, a copper-free click reaction (14). Based

on our results showing that IL-2R α is localized primarily to the nucleus, we focused on the nuclear fraction. IL-2R α protein was isolated by immunoprecipitation using the anti-IL-2R α from BosterBio, and then detected with either the anti-IL-2R α from BosterBio or an anti-IL-2R α (phospho-ser 268). Levels of DBCO-labeled IL-2R α , assessed by densitometry, were normalized based on either total protein or total IL-2R α protein per band. Normalizing with total IL-2R α protein was sometimes difficult since the DBCO label variably impacted recognition of IL-2R α (Supplementary Figure 3). Based on 3 separate experiments, the half-life of IL-2R α was 8.4 ± 2.5 days (Figure 8). These results demonstrate that the half-life of IL-2R α is longer than most cellular proteins and may explain the discrepancy between levels of *IL2RA* DNA and protein observed in IL-2R α KO mice.

IL-2Ra KO VSMC

Responses of IL-2R α KO VSMC to sera, evident in routine culture, began to give us insight into the differences between WT and KO VSMC. Doubling times were significantly shorter in KO vs WT VSMC (Figure 9). KO VSMC were also much smaller than WT and took up less DAPI; these differences were heightened upon stimulation with FBS (Figure 9). The latter observations are consistent with the finding that DNA content is directly proportional to cell size (35). In comparing nuclear area and DNA content of WT and KO VSMC, however, we noted that the decrease in DNA content was out of proportion to the decrease in nuclear area. KO nuclei were approximately half the size of WT, but only had 1/6 the amount of DNA. This finding suggests that KO

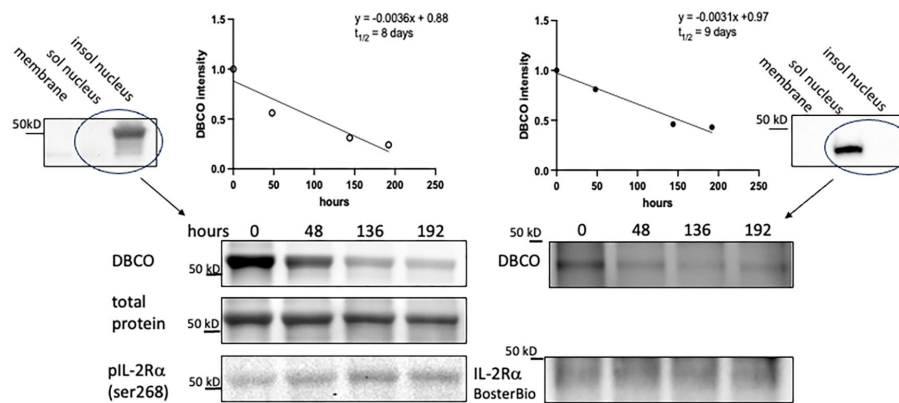


FIGURE 8

IL-2R α exhibits a prolonged half-life. VSMC were labeled with AHA-containing, methionine free media for 48h then chased with complete media for the durations above. IL-2R α was then isolated by immunoprecipitation with anti-IL-2R α from BosterBio. AHA-labeled IL-2R α was detected by DBCO-488 and total IL-2R α was detected using anti-IL-2R α , anti-phospho IL-2R α ser268, or total protein stain as indicated. DBCO intensities, normalized to total IL-2R α , were graphed on a linear scale and linear regression analysis was performed to determine the protein half-life. Blots at the left and right edges of the figure show VSMC fractionated into membrane, soluble nuclear, and insoluble nuclear fractions (both nuclear fractions digested with Benzonase[®]) and probed with antibodies as indicated. Circled lanes indicate the fractions that were combined for immunoprecipitation. The half-life on the left hand side of the figure was calculated using the band detected by anti-phospho IL-2R α ser268 and total protein (of that band) for normalization. The half-life on the right hand side of the figure was calculated using the band detected by anti-IL-2R α from BosterBio and immunodetection for normalization. In the above experiments, immunoprecipitated IL-2R α was eluted using a denaturing buffer. Use of a non-denaturing buffer yielded a similar half-life of 8.25 days.

VSMC are hypodiploid, which implies a severe dysregulation of cell proliferation and/or division. Hypodiploid cells are mainly associated with an aggressive form of acute lymphoblastic leukemia (36, 37).

Discussion

Knock out mice are often used to determine the function of a protein. Both IL-2 and IL-2R α KO mice were instrumental in determining that the IL-2/IL-2R system plays a major regulatory role in the immune system by promoting the survival of T regulatory cells and through activation-induced cell death (1, 3, 38). Our results show that IL-2R α is diminished, but not absent, in IL-2R α KO mice. Furthermore, our data suggest that the source of IL-2R α is maternal microchimerism. The infertility of IL-2R α KO mice, mandating a heterozygous mother, combined with the long half-life of IL-2R α , creates a unique situation in which substantial amounts of IL-2R α are present in KO mice. The predominantly nuclear localization of IL-2R α , reported here, is likely responsible for its lack of detection before now.

Our studies of IL-2R α KO mice and the mechanisms contributing to its incomplete elimination have led to several remarkable discoveries including: (1) IL-2R α is localized primarily to the nucleus, (2) IL-2R α protein has a long half-life, and (3) IL-2R α is transmitted between cells. First, and foremost, is our observation that IL-2R α is localized primarily to the nucleus. Prior reports addressing the potential nuclear localization of IL-2R subunits are rare. In 1988, Jothy, et al. showed that IL-2R α was transiently localized to the nucleus of concanavalin A supernatant-stimulated HT-2 cells (39). Conversely, Fujii, et al, showed that neither IL-2R β nor IL-15R α could be transported to the nucleus, however they did not test IL-2R α (40). Our report adds to this

literature, clearly demonstrating that IL-2R α localizes to the nucleus. In this location, our data show that IL-2R α deficient cells become smaller and lose DNA when stimulated to proliferate. These results are consistent with our finding that quiescent and senescent cells have increased nuclear IL-2R α relative to proliferating cells (unpublished observation). While not formally studied, our methods also intimate that IL-2R α binds DNA, given that we were unable to immunoprecipitate IL-2R α without first digesting DNA. Taken together, these findings suggest that IL-2R α contributes to the regulation of cell division and/or acts as a transcription factor.

In addition to its nuclear localization, we have also determined that IL-2R α has a long half-life relative to most proteins. Systematic studies of protein half lives in cells and tissues have shown that mitochondrial and nuclear proteins have the longest half-lives, consistent with the predominantly nuclear localization of IL-2R α reported here (33, 41). Proteins with long half-lives tend to play key structural or functional roles within cells. Histones, for example, with half-lives ranging from 15 days in dividing cells to 240+ in non-dividing cells, contribute to the organization of chromatin which in turn regulates cell division, DNA damage responses, gene expression, and cell fate (33, 42, 43). Several mitochondrial proteins have half-lives on the order of 7 days; these longer-lived proteins were found to contribute to the stability of the electron transport chain (44). The long half-life of IL-2R α , demonstrated here, provides additional support to the concept that IL-2R α has a newfound, fundamental role in regulating cell size and proliferation.

Finally, our investigation into the incomplete elimination of IL-2R α in IL-2R α KO mice revealed that IL-2R α is shared/transported between cells. In our experiments, cell contact was not required for transmission, however this does rule out the possibility that sharing via cell contact also occurs. Sharing of IL-2R α in the absence of cell

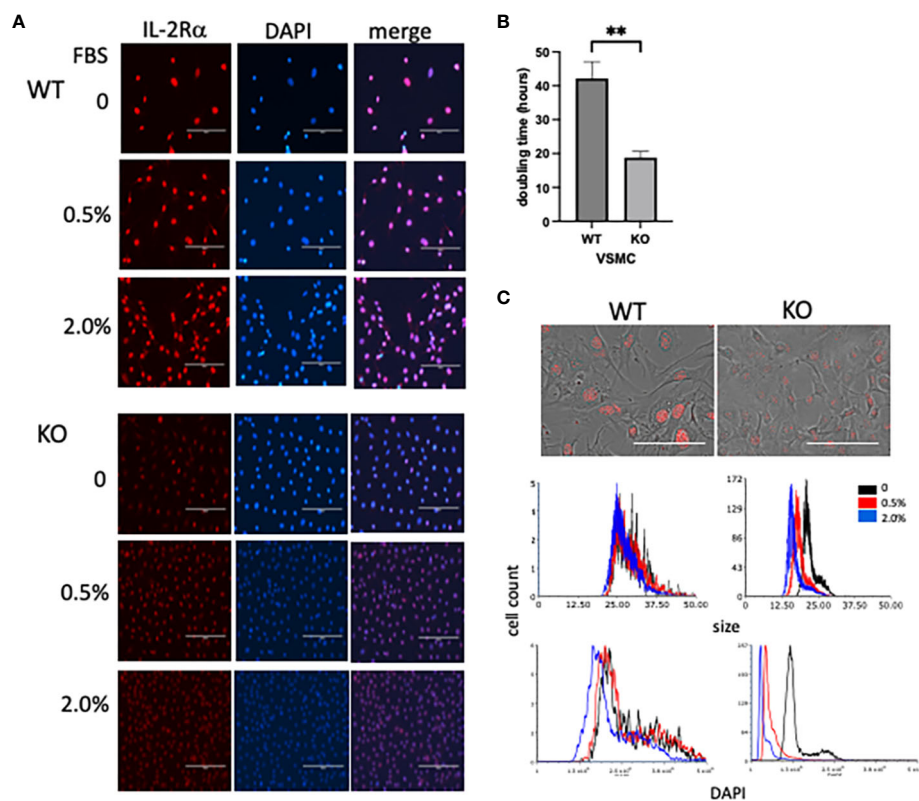


FIGURE 9

IL-2R α KO VSMC are small and hypodiploid. (A) VSMC, isolated from IL-2R α WT and KO mice, were cultured for 72h in serum free media with increasing concentrations of FBS. Cells were probed for IL-2R α expression using the anti-IL-2R α from Boster as described in Figure 1. Scale bar = 200 μ . (B) Doubling times of WT and KO VSMC were calculated using three time points over 72h (34). Data represent average \pm SEM of 5 separate experiments. (C, top) Phase and IL-2R α overlay images from WT and KO VSMC in serum free media and probed for IL-2R α as in (A). Scale bar = 100 μ . (C, middle and bottom) Nuclei of VSMC from (A) were imaged for area and DAPI intensity using a Cytation imaging plate reader (Biotek). Data accrued from these images were then processed using flow cytometry software. Results shown are representative of 3 (A, C) separate experiments or 5 (B) collated experiments. ** $P \leq 0.01$.

contact suggests that IL-2R α was transported through extracellular vesicles such as an exosomes or apoptotic bodies. Extracellular vesicles are a major means of intercellular communication and have been shown to participate in many biological processes including differentiation, proliferation, apoptosis, motility, and others (31). If IL-2R α plays a cell intrinsic role in regulating proliferation, as suggested by our findings, then transmission of IL-2R α by its “producers” may promote the normal function of surrounding KO cells and attenuate the consequences of IL-2R α deficiency.

As previously described, we used G418 resistance to decrease the production of IL-2R α , originating from IL-2R α heterozygous cells, in VSMC isolated from IL-2R α KO mice. This method was partially successful (Figures 6, 7); however, to date we have not been able to completely eradicate IL-2R α . Reasons for this ongoing incomplete eradication likely include (1) insufficient difference between G418 resistance of homozygous vs heterozygous cells, (2) lack of means to detect and exclude live IL-2R α producing cells, and (3) techniques such as clonal dilution are challenging in primary VSMC as their viability at the single cell level is poor. Our laboratory is in the process of finding other methods of detecting and eliminating IL-2R α producing cells to establish a complete IL-2R α KO phenotype both *in vitro* and *in vivo*.

In summary, our data reveals the surprising finding that IL-2R α KO mice express significant amounts of IL-2R α protein. Our initial assessment of IL-2R α KO VSMC suggests that IL-2R α , localized to the nucleus and independent of IL-2, plays an unexpected role in the regulation of cell proliferation.

Data availability statement

The raw data supporting the conclusions of this article will be made available by the authors, without undue reservation.

Ethics statement

The requirement of ethical approval was waived by Institutional Review Board at Wright State University for the studies on humans because tissues were obtained from deceased organ donors who are not considered human subjects by the HHS in the context of research. The studies were conducted in accordance with the local legislation and institutional requirements. Written informed consent for research was provided by next of kin. Human tissues

were handled in accord with the Wright State University Institutional Biosafety Committee.

Author contributions

VW: Data curation, Methodology, Writing – review & editing. KD: Data curation, Methodology, Writing – review & editing. GC: Data curation, Methodology, Writing – review & editing. LW: Conceptualization, Funding acquisition, Investigation, Project administration, Supervision, Writing – original draft, Writing – review & editing.

Funding

The author(s) declare that financial support was received for the research, authorship, and/or publication of this article. These studies were supported by a grant from the National Institutes of Health (R03AG068696) and from the Boonshoft School of Medicine at Wright State University to LW.

Acknowledgments

The authors would like to extend a heartfelt thanks to the Microarray and Microbiome Sequencing Core Facility at University

of Texas Southwestern Medical Center for performing the quantitative PCR experiments and targeted genomic sequencing assay for the present study.

Conflict of interest

The authors declare that the research was conducted in the absence of any commercial or financial relationships that could be construed as a potential conflict of interest.

Publisher's note

All claims expressed in this article are solely those of the authors and do not necessarily represent those of their affiliated organizations, or those of the publisher, the editors and the reviewers. Any product that may be evaluated in this article, or claim that may be made by its manufacturer, is not guaranteed or endorsed by the publisher.

Supplementary material

The Supplementary Material for this article can be found online at: <https://www.frontiersin.org/articles/10.3389/fimmu.2024.1369818/full#supplementary-material>

References

1. Willerford DM, Chen J, Ferry JA, Davidson L, Ma A, Alt FW. Interleukin-2 receptor alpha chain regulates the size and content of the peripheral lymphoid compartment. *Immunity*. (1995) 3:521–30. doi: 10.1016/1074-7613(95)90180-9
2. Malek TR, Castro I. Interleukin-2 receptor signaling: at the interface between tolerance and immunity. *Immunity*. (2010) 33:153–65. doi: 10.1016/j.immuni.2010.08.004
3. Toomer KH, Lui JB, Altman NH, Ban Y, Chen X, Malek TR. Essential and non-overlapping IL-2R α -dependent processes for thymic development and peripheral homeostasis of regulatory T cells. *Nat Commun*. (2019) 10. doi: 10.1038/s41467-019-08960-1
4. Sharma R, Zheng L, Deshmukh US, Jarjour WN, Sung SJ, Fu SM, et al. Cutting edge: A regulatory T cell-dependent novel function of CD25 (IL-2R α) controlling memory CD8+ T cell homeostasis. *J Immunol*. (2007) 178:1251–5. doi: 10.4049/jimmunol.178.3.1251
5. Sharma R, Bagavant H, Jarjour WN, Sung S-J, Ju S-T. The role of fas in the immune system biology of IL-2R α . Knockout mice: interplay among regulatory T cells, inflammation, hemopoiesis, and apoptosis. *J Immunol*. (2005) 175:1965–73. doi: 10.4049/jimmunol.175.3.1965
6. García de Galdeano A, Boyano D, Smith-Zubiaga I, Cañavate L. B16F10 murine melanoma cells express interleukin-2 and a functional interleukin-2 receptor. *Tumor Biol*. (1996) 17:155–67. doi: 10.1159/000217978
7. Kronin V, Vremec D, Shortman K. Does the IL-2 receptor alpha chain induced on dendritic cells have a biological function? *Int Immunol*. (1998) 10:237–40. doi: 10.1093/intimm/10.2.237
8. Von Bergwelt-Baildon MS, Popov A, Saric T, Chemnitz J, Classen S, Stoffel MS, et al. CD25 and indoleamine 2,3-dioxygenase are up-regulated by prostaglandin E2 and expressed by tumor-associated dendritic cells *in vivo*: additional mechanisms of T-cell inhibition. *Blood*. (2006) 108:228–37. doi: 10.1182/blood-2005-08-3507
9. Arumugam P, Carroll KL, Berceci SA, Barnhill S, Wrenshall LE. Expression of a functional IL-2 receptor in vascular smooth muscle cells. *J Immunol*. (2019) 202:694–703. doi: 10.4049/jimmunol.1701151
10. Kwartler C, Zhou P, Kuang S-Q, Duan X-Y, Gong L, Milewicz D. Vascular smooth muscle cell isolation and culture from mouse aorta. *Bio-Protocols*. (2016) 6. doi: 10.21769/BioProtoc.2045
11. Libby P, O'Brien KV. Culture of quiescent arterial smooth muscle cells in a defined serum-free medium. *J Cell Physiol*. (1983) 115:217–23. doi: 10.1002/jcp.1041150217
12. Protocol 22371 - *Il2ra<tm1Dw>*. The Jackson Laboratory. Available at: <https://www.jax.org/Protocol?stockNumber=002952&protocolID=22371>.
13. Morey TM, Esmaeili MA, Duennwald ML, Rylett RJ. SPAAC pulse-chase: A novel click chemistry-based method to determine the half-life of cellular proteins. *Front Cell Dev Biol*. (2021) 9. doi: 10.3389/fcell.2021.722560
14. Lutz J-F. Copper-free azide-alkyne cycloadditions: new insights and perspectives. *Angew Chem IntEd*. (2008) 47:2182–4. doi: 10.1002/anie.200705365
15. Agard NJ, Prescher JA, Bertozzi CR. A strain-promoted [3 + 2] azide-alkyne cycloaddition for covalent modification of biomolecules in living systems. *J Am Chem Soc*. (2004) 126:15046–7. doi: 10.1021/ja044996f
16. Senichkin V, Prokhorova E, Zhivotovsky B, Kopeina G. Simple and efficient protocol for subcellular fractionation of normal and apoptotic cells. *Cells*. (2021) 10:1–13. doi: 10.3390/cells10040852
17. Van Geel R, Pruijn GJM, Van Delft FL, Boelens WC. Preventing thiol-ene addition improves the specificity of strain-promoted azide-alkyne cycloaddition. *Bioconjug Chem*. (2012) 23:392–8. doi: 10.1021/bc200365k
18. 002952 - *IL-2R α -J Strain Details*. The Jackson Laboratory. Available at: <https://www.jax.org/strain/002952>.
19. Rubin LA, Kurman CC, Fritz ME, Biddison WE, Boutin B, Yarchoan R, et al. Soluble interleukin 2 receptors are released from activated human lymphoid cells *in vitro*. *J Immunol*. (1985) 135:3172–7. doi: 10.4049/jimmunol.135.5.3172
20. Russell SE, Moore AC, Fallon PG, Walsh PT. Soluble IL-2R α (sCD25) exacerbates autoimmunity and enhances the development of Th17 responses in mice. *PLoS One*. (2012) 7:e47748. doi: 10.1371/journal.pone.0047748
21. Thierry-Mieg J, Thierry-Mieg D. AceView: a comprehensive cDNA-supported gene and transcripts annotation. *Genome Biol*. (2006) 7:S12. doi: 10.1186/gb-2006-7-s1-s12
22. McHugh RS, Shevach EM. Cutting edge: depletion of CD4+CD25+ Regulatory T cells is necessary, but not sufficient, for induction of organ-specific autoimmune disease. *J Immunol*. (2002) 168:5979–83. doi: 10.4049/jimmunol.168.12.5979

23. Setiady YY, Coccia JA, Park PU. *In vivo* depletion of CD4+FOXP3+ Treg cells by the PC61 anti-CD25 monoclonal antibody is mediated by Fc γ RIII+ phagocytes. *Eur J Immunol.* (2010) 40:780–6. doi: 10.1002/eji.200939613
24. Kraft ARM, Wlodarczyk MF, Kenney LL, Selin LK. PC61 (anti-CD25) treatment inhibits influenza A virus-expanded regulatory T cells and severe lung pathology during a subsequent heterologous lymphocytic choriomeningitis virus infection. *J Virol.* (2013) 87:12636–47. doi: 10.1128/JVI.00936-13
25. Solomon I, Amann M, Goubier A, Arce Vargas F, Zervas D, Qing C, et al. CD25-Treg-depleting antibodies preserving IL-2 signaling on effector T cells enhance effector activation and antitumor immunity. *Nat Cancer.* (2020) 1:1153. doi: 10.1038/s43018-020-00133-0
26. Su E, Johnson K, Tighioart H, Bianchi D. Murine maternal cell microchimerism: analysis using real-time PCR and *in vivo* imaging. *Biol Reprod.* (2008) 78:883–7. doi: 10.1095/biolreprod.107.063305
27. Stelzer IA, Thiele K, Solano ME. Maternal microchimerism: Lessons learned from murine models. *J Reprod Immunol.* (2015) 108:12–25. doi: 10.1016/j.jri.2014.12.007
28. Schepanski S, Chini M, Sternemann V, Urbschat C, Thiele K, Sun T, et al. Pregnancy-induced maternal microchimerism shapes neurodevelopment and behavior in mice. *Nat Commun.* (2022) 13. doi: 10.1038/s41467-022-32230-2
29. Wrenshall LE, Stevens ET, Smith DR, Miller JD. Maternal microchimerism leads to the presence of interleukin-2 in interleukin-2 knock out mice: Implications for the role of interleukin-2 in thymic function. *Cell Immunol.* (2007) 245:80–90. doi: 10.1016/j.cellimm.2007.04.002
30. Dutta P, Molitor-Dart M, Bobadilla JL, Roenneburg DA, Yan Z, Torrealba JR, et al. Microchimerism is strongly correlated with tolerance to noninherited maternal antigens in mice. *Blood.* (2009) 114:3578–87. doi: 10.1182/blood-2009-03-213561
31. Liu Y-J, Wang C. A review of the regulatory mechanisms of extracellular vesicles-mediated intercellular communication. *Cell Commun Signal.* (2023) 21:77. doi: 10.1186/s12964-023-01103-6
32. Caruso S, Poon IKH. Apoptotic cell-derived extracellular vesicles: More than just debris. *Front Immunol.* (2018) 9. doi: 10.3389/fimmu.2018.01486
33. Chen W, Smeekens JM, Wu R. Systematic study of the dynamics and half-lives of newly synthesized proteins in human cells. *Chem Sci.* (2016) 7:1393–400. doi: 10.1039/C5SC03826J
34. Roth V. Doubling Time Calculator (2006). Available online at: https://www.doubling-time.com/compute_more.php.
35. Gillooly JF, Hein A, Damiani R. Nuclear DNA content varies with cell size across human cell types. *Cold Spring Harb Perspect Biol.* (2015) 7:1–27. doi: 10.1101/cshperspect.a019091
36. Safavi S, Forestier E, Golovleva I, Barbany G, Nord KH, Moorman AV, et al. Loss of chromosomes is the primary event in near-haploid and low-hypodiploid acute lymphoblastic leukemia. *Leukemia.* (2013) 27:248–50. doi: 10.1038/leu.2012.227
37. Safavi S, Paulsson K. Near-haploid and low-hypodiploid acute lymphoblastic leukemia: Two distinct subtypes with consistently poor prognosis. *Blood.* (2017) 129:420–3. doi: 10.1182/blood-2016-10-743765
38. Kundig T, Schorle H, Bachmann M, Hengartner H, Zinkernagel R, Horak I. Immune responses in interleukin-2-deficient mice. *Sci (80-).* (1993) 262:1059–61. doi: 10.1126/science.8235625
39. Jothy S, Abadie A, Froussard P, Duphot M, Thèze J. Nuclear location of the p55 subunit of the IL-2 receptor following activation of the HT-2 T helper cell line. *Ann Inst Pasteur Immunol.* (1988) 139:237–44. doi: 10.1016/0769-2625(88)90137-7
40. Fujii H, Hoshino A. Lack of nuclear translocation of cytoplasmic domains of IL-2/IL-15 receptor subunits. *Cytokine.* (2008) 46:302–8. doi: 10.1016/j.cyto.2009.02.014
41. Price JC, Guan S, Burlingame A, Prusiner SB, Ghaemmaghami S. Analysis of proteome dynamics in the mouse brain. *Proc Natl Acad Sci.* (2010) 107:14508–13. doi: 10.1073/pnas.1006551107
42. Mathieson T, Franken H, Kosinski J, Kurzawa N, Zinn N, Sweetman G, et al. Systematic analysis of protein turnover in primary cells. *Nat Commun.* (2018) 9. doi: 10.1038/s41467-018-03106-1
43. Shmueli MD, Sheban D, Eisenberg-Lerner A, Merbl Y. Histone degradation by the proteasome regulates chromatin and cellular plasticity. *FEBS J.* (2022) 289:3304–16. doi: 10.1111/febs.15903
44. Krishna S, Arrojo Drigo R, Capitano JS, Ramachandra R, Ellisman M, Hetzer MW. Identification of long-lived proteins in the mitochondria reveals increased stability of the electron transport chain. *Dev Cell.* (2021) 56:2952–65. doi: 10.1016/j.devcel.2021.10.008